

# AGE AND GEOCHEMISTRY OF LATE PRECAMBRIAN SEDIMENTS OF THE HAMMAMAT SERIES FROM THE NORTHEASTERN DESERT OF EGYPT

K.M. WILLIS\* and R.J. STERN

*University of Texas at Dallas, Richardson, TX 75080 (U.S.A.)*

N. CLAUER

*Centre de Sédimentologie et Géochimie de la Surface (CNRS), Université L. Pasteur, 67084 Strasbourg (France)*

(Received June 2, 1987; revision accepted April 11, 1988)

## Abstract

Willis, K.M., Stern, R.J. and Clauer, N., 1988. Age and geochemistry of Late Precambrian sediments of the Hammamat Series from the Northeastern Desert of Egypt. *Precambrian Res.*, 42: 173–187.

Late Precambrian crustal evolution in the Northeastern Desert of Egypt culminated in a major episode of strong extension, accompanied by bimodal igneous activity and deposition of clastic sediments in restricted terrigenous basins. These sediments, known as the Hammamat Series, record the uncovering of the evolving crust of the region. We have undertaken petrographic, geochemical, and Rb–Sr and K–Ar geochronologic studies of Hammamat samples collected along a single traverse. The lower half of a 400 m thick section consists of coarse detritus shed from nearby ensimatic terranes, while the upper half was derived from rapid reworking of bimodal igneous rocks similar to those of the Dokhan Volcanics and Pink Granites, units that are preserved within the region.

Rb–Sr whole-rock analyses give an 8-point isochron age of  $585 \pm 15$  Ma with an initial  $^{87}\text{Sr}/^{86}\text{Sr}$  of  $0.70323 \pm 0.00013$ , interpreted to approximate closely the time of sedimentation. This is very similar to the K–Ar ages of the coarser clay fractions ( $2\text{--}0.5 \mu\text{m}$ ) ( $588\text{--}567$  Ma). This result is consistent with stratigraphic considerations and other geochronological studies indicating that Hammamat deposition occurred at  $\sim 590$  Ma.

Rb–Sr analyses of leached and unleached size fractions indicate thermal resetting at  $524 \pm 17$  Ma accompanied or followed by fluxing of a radiogenic Sr-rich pore fluid ( $^{87}\text{Sr}/^{86}\text{Sr} = 0.7124$ ). This is further indicated by K–Ar ages of the  $0.2\text{--}0.5 \mu\text{m}$  size fraction of  $542\text{--}532$  Ma.

## Introduction

The formation of the continental crust in Northeast Africa and Arabia occurred during the last 400 Ma of the Precambrian (Pan-African event, as defined by Gass, 1977, and

Kröner, 1984). Much of the crustal growth in Afro-Arabia apparently occurred as arc and back-arc basin systems coalesced into proto-continental 'terrane' which were then sutured together (Kröner, 1985; Stoesser and Camp, 1985). In northernmost Egypt, however, crustal growth during  $600\text{--}575$  Ma occurred in an extensional tectonic environment (Stern et al., 1984). The most important lines of evidence for

\*Current address: Sun Exploration and Production Company, Box 2880, Dallas, TX 75221, U.S.A. (Formerly K.W. Massey.)

the latter model include: (1) bimodal igneous activity characteristic of rifting, including the Dokhan Volcanics and the Pink Granite (Ressetar and Monrad, 1983; Stern and Gottfried, 1986); (2) subparallel bimodal and composite dike swarms, locally comprising up to 50% of the basement (Schürmann, 1966); (3) development of a transform system trending parallel to the extension direction (Stern, 1985); and (4) clastic sediments interpreted to have been deposited in rift basins (Grothaus et al., 1979).

The rift-related sedimentary succession is known as the Hammamat Series (Hume, 1934) named after the pharaonic quarries in Wadi Hammamat. These sediments are common in the Northern and Central Eastern Desert, becoming less common until they disappear completely south of 25°N (Fig. 1). These sediments are compositionally and texturally immature, reflecting deposition close to their provenance.

The resultant facies variations make it unlikely that a regional stratigraphy can be developed. In general, however, one or more of the following lithological characteristics serve to distinguish the Hammamat from other basement sedimentary sequences: (1) interbedded green and purple wackes, siltstones and shales; (2) breccias and conglomerates containing a variety of clasts, including the Dokhan Volcanics; and (3) conglomerates containing cobbles of Pink Granite (Andrew, 1939; Hafez and Abdel-Khalek, 1972; Grothaus et al., 1979). These sediments can be either undeformed or highly deformed. Not only do they carry cobbles of the Pink Granite, but they are also intruded by these plutons (Ries et al., 1983; Abuzeid, 1984). Clearly, the sediments of the Hammamat Series record a vigorous and important stage in the formation of the crust of northernmost Afro-Arabia.

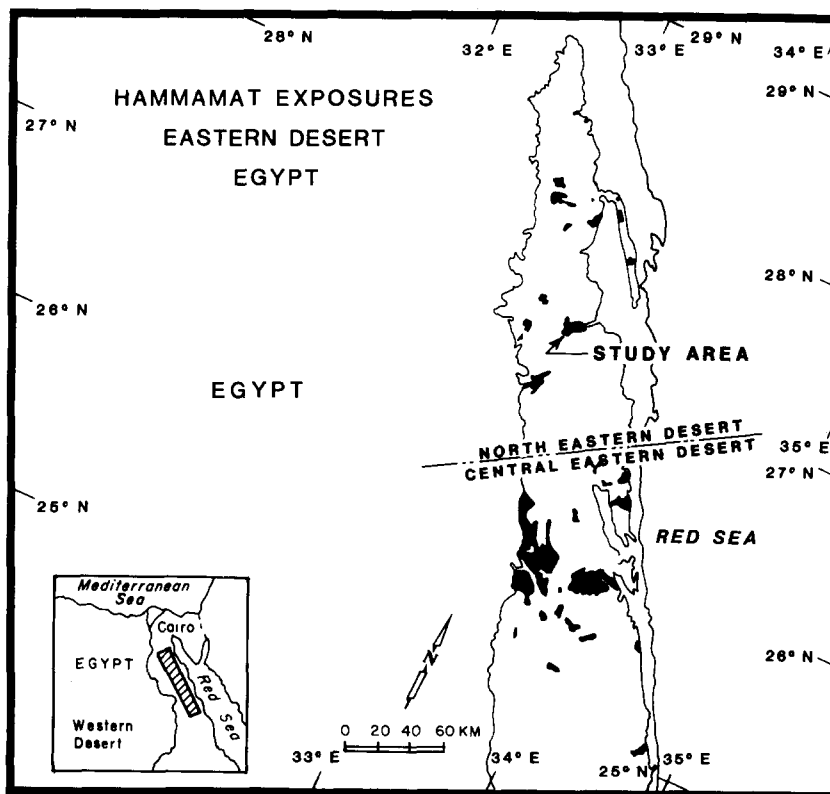


Fig. 1. Location of the Hammamat exposures in the Eastern Desert of Egypt (modified after El Ramly, 1972).

## Geologic setting

The study area lies within and just west of the Gebel Qattar and Gebel Dokhan areas in the Northeastern Desert of Egypt (Fig. 1), mapped at 1:50 000 by Ghobrial and Lotfi (1967). These authors interpreted the geologic history of the region to consist of the following events, from oldest to youngest: (1) deposition of clastic sediments, (2) eruption of the Dokhan Volcanics, and (3) intrusion of a variety of granite plutons and bimodal dike swarms. They also noted the many similarities between the Hammamat Series and the sediments of the Qattar–Dokhan area that were identified as Hammamat by Barthoux (1922), Hume (1934) and Ghanem et al. (1973).

The igneous rocks have been dated using Rb–Sr whole-rock and U–Pb zircon techniques

(Stern and Hedge, 1985). The Dokhan Volcanics conformably overlie the Hammamat and give a Rb–Sr whole-rock age of  $592 \pm 26$  Ma ( $2\sigma$ ). The Salah El Belih granodiorite, which intrudes the Hammamat and is cut by dikes, gives a zircon model age of 583 Ma. The dikes, which cut the Hammamat and may have been feeders for the Dokhan, give a Rb–Sr whole-rock age of  $598 \pm 8$  Ma. The youngest intrusive is the granite of Gebel Qattar at 579 Ma (zircon model age). The Hammamat sediments thus cannot be younger than 590 Ma in this region, and the conformable nature of the Hammamat–Dokhan contact suggests that it is probably not much older than 600–590 Ma. This estimate corresponds to the bracketed age of  $590 \pm 11$  Ma to  $619 \pm 9$  Ma for the Hammamat at  $26^\circ$  N (Ries et al., 1983).

Samples were collected in the course of a de-

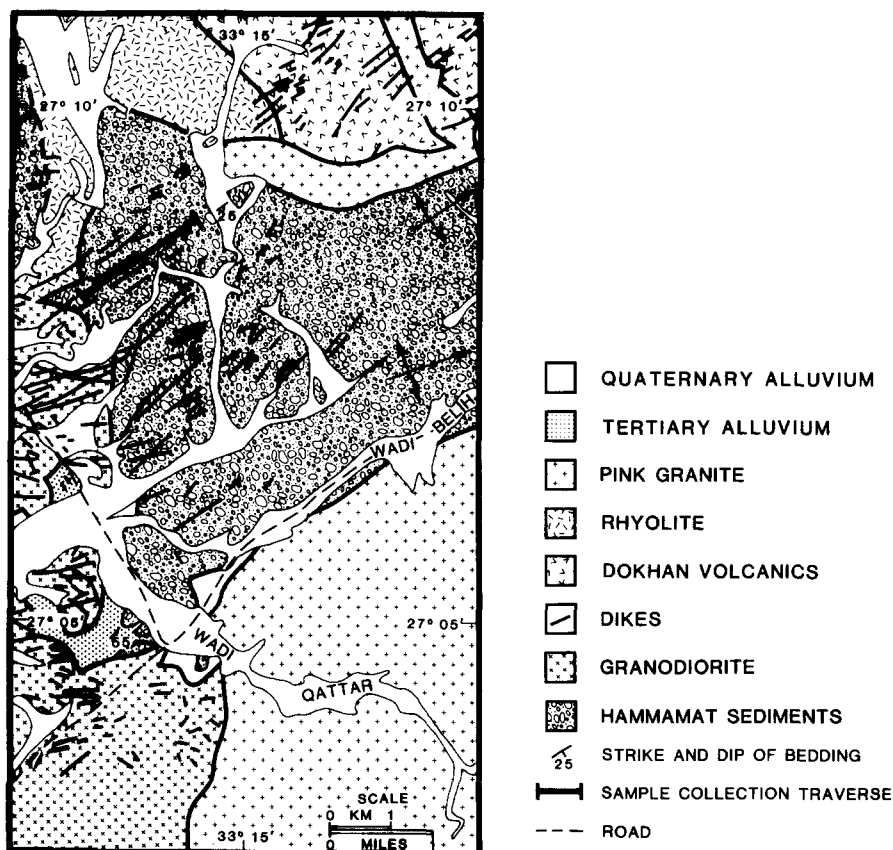


Fig. 2. Geologic map of the studied area.

tailed traverse near the western edge of the Hammamat exposures between Gebel Dokhan and Gebel Qattar (Fig. 2). This traverse was chosen to avoid the younger dikes and provide good exposures.

### Stratigraphy and petrography

The studied section is ~400 m thick with the base intruded everywhere by the Salah El Belih granodiorite. The lower half of the section consists of massive polymict breccias containing clasts of diorite, gabbro, and rare pink granite, green metasediments, and basaltic to andesitic volcanics (Fig. 3). Sandy interbeds become more common upsection. This is succeeded by a distinctive tuffaceous shale (samples E-220I, -K, -L) and another 50 m of breccia. About 50 m of occasionally cross-bedded arenite follows (E-220O, -Q, -R) and grades into 50 m of tuffaceous shale and siltstone (E-198H; E-220S, -U, -Y). This is then succeeded by 40 m of breccia and conglomerate containing abundant clasts of pink granite. This conglomerate is fi-

nally conformably overlain by the first of the Dokhan lavas (E-220Z of Stern and Gottfried, 1986).

Inspection of the clast population from the polymict breccias indicates that the source of the lower part of the section was composed of gabbros, diorites, mafic to felsic volcanics, and immature wackes. A representative count of clasts at several exposures gave: 19–31% gabbro and diorite, 19–45% wackes, 8–19% volcanics, and 2–5% vein quartz and granite. We interpret these to have been derived from a source similar to that of the ensimatic terrane of the Central Eastern Desert (Stern, 1981). The occurrence of rare clasts of red jasper, similar to jaspers associated with the banded iron formations of the Central Eastern Desert (Sims and James, 1984) is particularly convincing.

For the purpose of further clarifying the provenance and alteration history of the samples, thin sections and X-ray diffraction studies were undertaken on the sandstones and shales. Detailed textural and mineralogical observations are given by Massey (1984). The most common component of the samples is clay (17–74%); with decreasing grain size the amount of lithic fragments decreases from 43% to 1% and clay content increases from 25% to 74%. Monocrystalline quartz is present in minor amounts ( $\leq 13\%$ ) and polycrystalline quartz is minimal ( $\leq 2\%$ ). All samples are much richer in plagioclase than K-feldspar. Using Pettijohn's (1957) classification, they range from lithic to feldspathic graywacke, becoming more feldspathic with decreasing grain size.

Evidence of recrystallization processes include: (1) up to 4% calcite cement in the coarse-grained sandstones, (2) partial replacement of calcite cement by diagenetic clay, (3) sericitization of feldspars, (4) interstitial clay filling pore space, and (5) alteration of lithic grains. Although no slaty cleavage or stress-related grain-alignment could be described, a greenschist facies metamorphism is indicated by the illite crystallinity indices (see below) and a mineral paragenesis which includes chlorite,

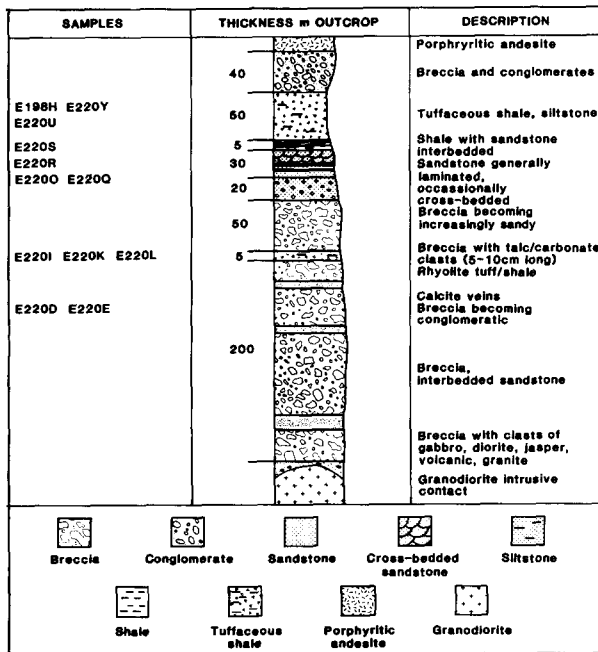


Fig. 3. Stratigraphic column of the Hammamat Series along the sample traverse.

epidote, actinolite, sericite, and albite. These features indicate that a post-depositional thermal event occurred, producing clay cement in between grains, authigenic mineral formation, and detrital grain alteration.

X-ray diffraction studies indicate that illite and chlorite are present in E220K and E220L, that chlorite and interlayered illite-smectite are present in E220S and E198H, and that kaolinite is systematically lacking. All illite is 2M polymorph, which may be interpreted as either a detrital or thermally reset form (Weaver, 1956). The illite crystallinity measurements determined after Kubler's method (1966) range between 2.8 and 3.6. They classify the samples within the epizone or greenschist facies. These results are in agreement with the presence of 2M polymorph which is the only polymorph stable within the range 200–350°C (Dunoyer de Segonzac, 1970).

## Geochemistry

A total of nine samples of sandstones, siltstones, and shales were analyzed for their concentrations of the major elements; one representative of each of these lithologies was analyzed for Ba and REE. Rb and Sr concentrations for seven of the samples were determined for the purposes of geochronology and are also listed here (Table I). These sediments show a restricted compositional range, especially in SiO<sub>2</sub> (60.6–67.4%), TiO<sub>2</sub> (0.61–0.99%), Al<sub>2</sub>O<sub>3</sub> (14.8–17.1%) and Fe<sub>2</sub>O<sub>3</sub> total (4.2–6.6%). The shales exhibit the largest compositional ranges, with enrichment of K<sub>2</sub>O (2.4–5.5%) and depletion of Na<sub>2</sub>O (0.56–3.0%) compared with the siltstones and sandstones (K<sub>2</sub>O=2.1–3.4%; Na<sub>2</sub>O=3.1–4.2%). Similarly, Rb concentrations are higher in the shales (77–140 ppm) than in the coarser clastics (63.5–89 ppm), while Sr is lower (51–479 ppm versus 369–757 ppm). K/Rb for all the sediments is remarkably constant (261–338). The shale is enriched in REE relative to the coarser sediments (Fig. 4), but has a markedly greater

Eu anomaly (Eu/Eu\* = 0.56 versus 0.70–0.83). Chondrite-normalized Ce/Yb ratios are very similar for the shale, the siltstone, and the sandstone ((Ce/Yb)<sub>n</sub> = 9.8–11.0). Ba is uniformly high (980–1090 ppm). These compositional features are very similar to those determined for the Hammamat in Wadi Hammamat to the south (Noweir and El-Din, 1979).

Table I also lists the calculated composition of the average upper Hammamat sediment from this area, based on the proportions of sandstone (45.5%), siltstone (45.5%), and shale (9%) estimated for the upper half of the section studied (note the absence of analyses for the lower breccias and uppermost conglomerate) and the mean composition for each lithology. The relatively high K<sub>2</sub>O (3.0%), Rb (79 ppm), Ba (1014 ppm), and LREE-enriched pattern ((Ce/Yb)<sub>n</sub> = 10.3) indicate that at least the upper part of this section was derived from a LIL- and LREE-enriched source. Plausible candidates for this enriched source include the Dokhan Volcanics and the Pink Granite, both of which occur as clasts in the conglomerates and breccias.

The possibility that the sediments of the upper half of the Hammamat section were largely derived from erosion and explosive eruption of the late Precambrian bimodal igneous rocks of the Northeastern Desert was investigated using a Wright–Doherty mixing program (Wright and Doherty, 1970). The compositions of the mean Dokhan andesite and Gattarian granite (= Pink Granite) are listed in Table I. The 'Average Hammamat Sediment' (hereafter, AHS) of Table I is well matched by a mixture of 71.7% andesite and 28.3% granite ( $\sum r^2 = 0.87$ ). Using these percentages and the trace element contents of the mean andesite and granite, the trace element signature of the sediment could be predicted; it generally corresponds well with that of the AHS. The REE patterns of the AHS and the mixing model are parallel ((Ce/Yb)<sub>n</sub> = 10.3 and 9.6 respectively) and have similar Eu anomalies (Eu/Eu\* = 0.76 and 0.72 respectively). The AHS, however, contains 10–20%

TABLE I

Chemical data from the Hammamat sediments

	220K <sup>a</sup>	220L <sup>b</sup>	220O <sup>c</sup>	220Q <sup>b</sup>	220R <sup>c</sup>	220S <sup>a</sup>	220U <sup>b</sup>	220Y <sup>b</sup>	198H <sup>d</sup>	Average <sup>d</sup> Hammamat	Dokhan <sup>e</sup> andesite	Qattar <sup>f</sup> granites	Mixing <sup>g</sup> model
<i>Major elements (wt.%)</i>													
SiO <sub>2</sub>	61.49	67.40	63.20	62.24	62.63	61.67	63.52	63.00	60.55	65.21	61.19	74.65	64.95
TiO <sub>2</sub>	0.80	0.76	0.64	0.99	0.61	0.75	0.72	0.79	0.68	0.75	1.11	0.20	0.86
Al <sub>2</sub> O <sub>3</sub>	16.02	14.76	15.55	14.99	14.91	17.10	16.05	17.08	17.00	16.06	16.26	13.52	15.49
Fe <sub>2</sub> O <sub>3</sub> T	6.63	4.71	4.57	6.81	4.17	5.82	4.79	5.21	5.86	5.14	6.25	1.62	4.95
MnO	0.14	0.06	0.10	0.12	0.17	0.08	0.09	0.08	0.11	0.12	0.09	0.04	0.08
MgO	3.22	2.37	2.28	2.81	1.74	2.50	2.20	2.33	4.00	2.38	3.00	0.26	2.23
CaO	3.04	1.90	3.51	2.98	5.14	1.79	2.88	3.17	0.79	3.49	4.88	0.97	3.78
Na <sub>2</sub> O	3.03	3.51	4.16	4.04	3.43	1.51	3.79	3.06	0.56	3.62	4.13	4.16	4.14
K <sub>2</sub> O	2.42	2.10	2.93	2.61	2.78	4.80	2.89	3.40	5.51	3.02	2.73	4.52	3.24
P <sub>2</sub> O <sub>5</sub>	0.23	0.19	0.19	0.25	0.20	0.25	0.19	0.21	0.20	0.21	0.36	0.06	0.28
LOI	2.66	2.10	2.83	2.37	4.05	3.15	2.06	2.28	4.02	-	-	-	-
Total	99.68	99.86	99.96	100.21	99.83	99.42	99.18	100.70	99.28	100.0	100.0	100.0	100.0
<i>Trace elements (ppm)</i>													
Rb	77	63.5	72	-	-	136	81	89	140	79	52	189	91
Sr	479	369	757	-	-	247	649	641	51	619	826	125	628
Ba	-	-	1030	-	-	1091	983	-	-	1014	725	433	642
Ce	-	-	57.8	-	-	78.7	63.3	-	-	62.1	65.0	79.5	69.1
Nd	-	-	27.3	-	-	35.3	28.0	-	-	28.3	33.3	34.0	33.5
Sm	-	-	4.93	-	-	6.47	5.09	-	-	5.14	6.24	6.83	6.41
Eu	-	-	1.04	-	-	1.08	1.26	-	-	1.14	1.69	0.66	1.40
Gd	-	-	3.95	-	-	5.14	4.00	-	-	4.08	4.93	5.73	5.16
Dy	-	-	3.06	-	-	4.19	3.23	-	-	3.24	3.43	5.50	4.02
Er	-	-	1.59	-	-	2.21	1.75	-	-	1.72	1.58	3.02	1.99
Yb	-	-	1.50	-	-	2.05	1.47	-	-	1.54	1.31	3.19	1.84
K/Rb	261	274	338	-	-	293	296	317	327	317	436	198	296
K/Ba	-	-	23.6	-	-	36.5	24.4	-	-	24.7	31.3	86.6	42
(Ce/Yb) <sub>N</sub>	-	-	9.8	-	-	9.8	11.0	-	-	10.3	12.6	6.3	9.6
Eu/Eu*	-	-	0.70	-	-	0.56	0.83	-	-	0.76	0.90	0.32	0.72

Fe<sub>2</sub>O<sub>3</sub>T = Total iron as Fe<sub>2</sub>O<sub>3</sub>. LOI = Loss on ignition. Major elements analyzed by XRF (S. Mertzman, Franklin and Marshall College). Trace elements by isotope dilution (see Stern and Gottfried, 1986 for methods).

<sup>a</sup>Shale. <sup>b</sup>Siltstone. <sup>c</sup>Sandstone.

<sup>d</sup>Average Hammamat Sediment, based on weighted average of the proportion of siltstone, sandstone, and shale in the upper half of the studied section (recalculated anhydrous).

<sup>e</sup>Mean of eight andesitic rocks from the Qattar-Dokhan area, recalculated anhydrous (Stern and Gottfried, 1986).

<sup>f</sup>Mean of four granites from the Qattar-Dokhan area, recalculated anhydrous (Stern and Gottfried, 1986).

<sup>g</sup>Best-fit mixture of 'Mean Dokhan Andesite' (71.7%) and 'Mean Pink Granite' (28.3%) as determined by Wright-Doherty major element model ( $r^2=0.87$ ). Trace element concentrations are based on the major element best fit.

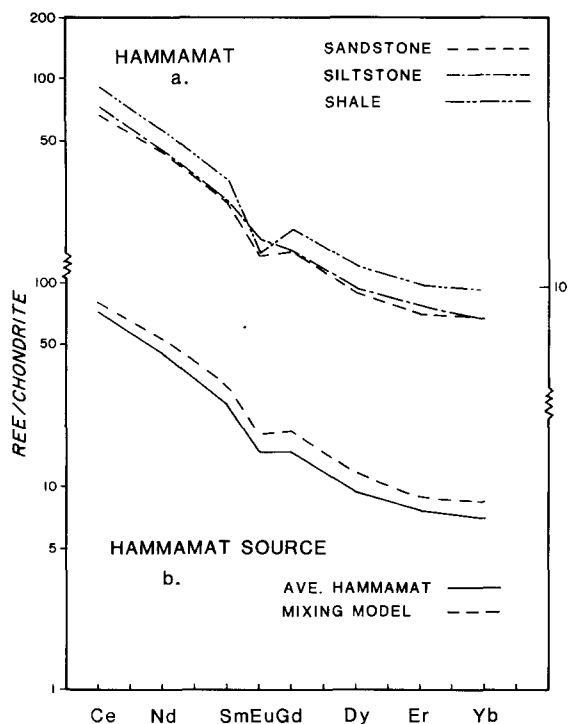


Fig. 4. REE patterns of the Hammamat lithologies and modeled source material. (a) Chondrite-normalized REE patterns, from Table I. (b) REE patterns for the modeled source compared with that of the calculated average (AVE) Hammamat.

less REE than that required by the mixing model (Fig. 3). These results indicate that, at least, the upper part of the Hammamat was predominantly derived from reworked Dokhan andesites and Pink Granite (and related rhyolites) in the proportion of  $\sim 3:1$ . This contrasts with the fact that the lower part of the section appears to be derived from a terrane more similar to that represented by the Central Eastern Desert. This older, more primitive component may also have contributed, to a lesser extent, to the upper part of the Hammamat, perhaps manifested in the lower REE content of the AHS compared with that predicted by the mixing model.

### Geochronology results

Rb, Sr amounts and Sr isotopic compositions were determined on whole rocks, clay size-fractionations,

a leachate and residues of these fractions after leaching with ammonium acetate, as well as two calcites from veins in the sedimentary sequence. After HF and HCl digestion and separation on cation exchange resins, Rb and Sr were measured on solid-source mass spectrometers. Details of the procedure have been described by Stern and Hedge (1985). All ratios are normalized to the usual constants; the  $\lambda^{87}\text{Rb}$  decay constant used for the age calculations is  $1.42 \times 10^{-11} \text{ a}^{-1}$  (Steiger and Jäger, 1977) and the program for these age calculations is from York (1966). The reproducibility of the Sr isotopic determination was periodically checked by determinations of the Eimer and Amend  $\text{SrCO}_3$  standard. During the course of this study, the  $^{87}\text{Sr}/^{86}\text{Sr}$  for this standard averaged  $0.70794 \pm 0.00009$  ( $2\sigma$ ) for four analyses.

The Rb–Sr results are compiled in Table II. Eight whole rocks were analyzed: one sandstone, two siltstones and five shales. Two calcite veins occurring in the sedimentary sequence were also studied. Five clay fractions were split into different size fractions following a procedure described by Thiry (1974), and subjected to leaching experiments similar to those of Morton and Long (1982). The clays were leached for 10 min in 25 ml cold ammonium acetate, centrifuged and analyzed as leachates and residues.

The eight whole rocks and the two calcites define a regression line on an isochron diagram (Fig. 5) with a date of  $585 \pm 15 \text{ Ma}$  ( $2\sigma$ ) for an initial  $^{87}\text{Sr}/^{86}\text{Sr}$  of  $0.70323 \pm 0.00013$  ( $2\sigma$ ) and a MSWD of 2.0. The untreated clay fractions fit along a second regression line with a steeper slope giving a date of  $643 \pm 15 \text{ Ma}$  with a very similar initial  $^{87}\text{Sr}/^{86}\text{Sr}$  of  $0.70310 \pm 0.00052$  (Fig. 6). The leachate of one clay fraction is far above both lines at about 0.712.

The preparation and analytical procedure of the K–Ar method is very similar to that presented by Bonhomme et al. (1975). The extraction line is made of Pyrex glass; the samples are preheated under vacuum at  $110^\circ\text{C}$  for several hours in order to lower the atmospheric Ar con-

TABLE II

Rb-Sr data

Sample	Sr (ppm)	Rb (ppm)	$^{87}\text{Rb}/^{86}\text{Sr}$	$^{87}\text{Sr}/^{86}\text{Sr}^a$
220I w.r.	472	62.1	0.380	$0.70664 \pm 13 \times 10^{-5}$
220K w.r.	479	77.0	0.465	$0.70681 \pm 14 \times 10^{-5}$
220K (1-0.5 $\mu\text{m}$ ) U	247	166	1.95	$0.7200 \pm 5 \times 10^{-5}$
220K (1-0.5 $\mu\text{m}$ ) R	203	166	2.36	$0.7216 \pm 4 \times 10^{-5}$
220K (0.5-0.2 $\mu\text{m}$ ) U	250	174	2.01	$0.7208 \pm 4 \times 10^{-5}$
220K (0.5-0.2 $\mu\text{m}$ ) R	170	174	2.97	$0.72515 \pm 12 \times 10^{-5}$
220L w.r.	369.1	63.5	0.498	$0.70731 \pm 7 \times 10^{-5}$
220O w.r.	757	72.0	0.276	$0.70559 \pm 7 \times 10^{-5}$
220S w.r.	247	136	1.60	$0.71639 \pm 7 \times 10^{-5}$
220S (1-0.5 $\mu\text{m}$ ) U	101	217	6.24	$0.76193 \pm 11 \times 10^{-5}$
220S (1-0.5 $\mu\text{m}$ ) R	54.5	215	11.4	$0.7954 \pm 4 \times 10^{-5}$
220S (0.5-0.2 $\mu\text{m}$ ) U	129	189	4.26	$0.74187 \pm 7 \times 10^{-5}$
220S (0.5-0.2 $\mu\text{m}$ ) R	47.8	196	11.9	$0.7924 \pm 4 \times 10^{-5}$
220U w.r.	649	80.9	0.361	$0.70610 \pm 11 \times 10^{-5}$
220U (1-0.5 $\mu\text{m}$ ) U	399	157	1.14	$0.71356 \pm 10 \times 10^{-5}$
220U (1-0.5 $\mu\text{m}$ ) R	309	159	1.49	$0.71470 \pm 9 \times 10^{-5}$
220Y w.r.	641	89.0	0.402	$0.70668 \pm 7 \times 10^{-5}$
220Y (1-0.5 $\mu\text{m}$ ) U	383	192	1.45	$0.71697 \pm 20 \times 10^{-5}$
198H w.r.	50.6	140	7.99	$0.77085 \pm 17 \times 10^{-5}$
198H (1-0.5 $\mu\text{m}$ ) U	128	183	4.14	$0.74049 \pm 17 \times 10^{-5}$
198H (1-0.5 $\mu\text{m}$ ) R	56.8	182	9.29	$0.77344 \pm 8 \times 10^{-5}$
198H (1-0.5 $\mu\text{m}$ ) L	-	-	0.095	$0.7124 \pm 5 \times 10^{-5}$
198H (0.5-0.2 $\mu\text{m}$ ) U	164	184	3.26	$0.73294 \pm 11 \times 10^{-5}$
E220E (C)	438	0.62	0.004	$0.70340 \pm 7 \times 10^{-5}$
E220D (C)	347	0.45	0.004	$0.70333 \pm 15 \times 10^{-5}$

$^{87}\text{Sr}/^{86}\text{Sr}$  normalized to E + A  $\text{SrCO}_3$   $^{87}\text{Sr}/^{86}\text{Sr} = 0.70800$ .

w.r. = Whole rock. Sizes in parentheses refer to size of particles analyzed. U = untreated, R = residue after leaching in 1 M ammonium acetate, L = leachate, (C) = calcite.

tamination. The reproducibility of the method has been controlled by periodic determinations of the standard GLO; during the course of the study, six determinations gave an average of  $24.77 \pm 0.24$  ( $2\sigma$ )  $\times 10^{-6}$   $\text{cm}^3 \text{g}^{-1}$  STP radiogenic  $^{40}\text{Ar}$ . The  $^{38}\text{Ar}$  spike used is from Clusius (Zürich) and the constants proposed by Steiger and Jäger (1977) have been used for age calculations. K was determined by flame spectrometry with a 1% accuracy. The reproducibility of the entire procedure is believed to be  $\sim 2\%$ . The K-Ar data are presented in Table III. Four whole rocks have apparent ages ranging from  $575 \pm 14$  to  $496 \pm 17$  Ma. Size fractions of five clay mixtures were also analyzed; the

values are widely scattered between  $588 \pm 13$  and  $309 \pm 7$  Ma.

### Geochronology discussion

All eight whole rocks fit on a single regression line. These results may be interpreted in two different ways:

(1) Based on the petrographic studies and mixing calculations already presented, the components of the Hammamat sedimentary sequence may be juvenile. Nevertheless, the whole rocks still record the age of the provenance and not the time of sedimentation. We believe that in special cases such as this where juvenile ma-

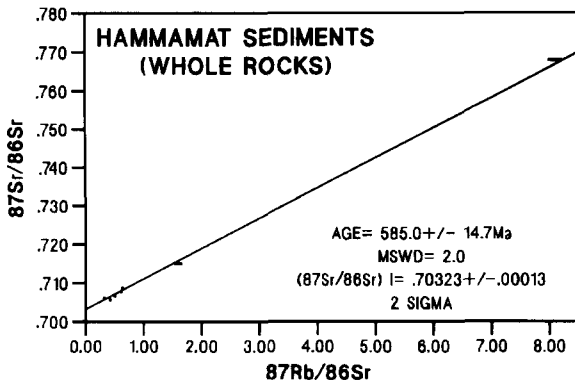


Fig. 5. Rb-Sr isochron diagram for the whole rocks (·) and two calcites (-).

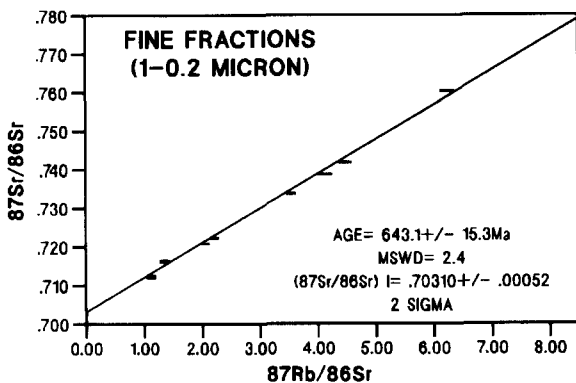


Fig. 6. Rb-Sr isochron diagram for the untreated clay fractions.

material is eroded and deposited very quickly after forming, it might be possible for the Rb-Sr whole-rock age to approximate the time of sedimentation. If this assumption is correct, the stratigraphic age of the sequence would be equal to or less than the 585 Ma given by the regression line.

(2) Based on petrographic and mineralogical observations, the regression line determined by the whole rocks could also be an isochron giving the age of a metamorphic event imprinted on the sediments by the granitic and granodioritic activities observed in the lower part of the sequence and giving ages close to that obtained here. Evidence of recrystallization processes have been described, such as calcite in veins and cement, a greenschist-facies mineral parage-

nesis, and clay crystallography suggesting temperatures above 200–250°C. If this interpretation is preferred, the two calcites which have  $^{87}\text{Sr}/^{86}\text{Sr}$  ratios indicative of the metamorphic migrating fluids should be used for the age calculation. In this case, the stratigraphic age of the Hammamat Series has to be considered as higher than the value given by the isochron.

The four K-Ar apparent ages on whole rocks range from  $574 \pm 14$  Ma, which is fairly close to the Rb-Sr whole-rock value, to  $496 \pm 17$  Ma. This lowering suggests a loss of radiogenic  $^{40}\text{Ar}$ , which might be attributable either to a continuous diffusive effect or to a later recrystallization event. As continuous diffusion of radiogenic  $^{40}\text{Ar}$  can no longer be considered as a general behavior in sediments (Clauer et al., 1984), it seems that a late event partly affected the K-Ar system of the whole rocks, without affecting their Rb-Sr system.

All coarser fractions of the clay components, the 1–2  $\mu\text{m}$  fractions of all samples and the 0.5–1  $\mu\text{m}$  fractions of some samples have K-Ar apparent ages clustering between  $588 \pm 13$  and  $567 \pm 12$  Ma, with a mean value at  $576 \pm 10$  Ma which agrees with the Rb-Sr age of  $585 \pm 15$  Ma for the whole rocks. These K-Ar results also emphasize the fact that no clay material could have been older than  $\sim 576$  Ma.

The intermediate clay size-fractions of 0.2–0.5 and 0.5–1  $\mu\text{m}$  have apparent K-Ar ages clustered between  $543 \pm 12$  and  $530 \pm 12$  Ma, with a mean value at  $535 \pm 5$  Ma. The two fractions  $< 0.2$   $\mu\text{m}$  gave surprisingly low K-Ar apparent ages with a mean value of  $326 \pm 18$  Ma.

The Rb-Sr data of the leaching experiments indicate that for all fractions, except for the 0.5–1  $\mu\text{m}$  fraction of 220S, the lines joining the untreated and residue fractions converge toward the leachate fraction measured for the 0.5–1  $\mu\text{m}$  fraction of 198H (Fig. 7). The fact that all lines have different slopes clearly indicates that leaching removed an easily exchangeable Sr from the clay particles having a  $^{87}\text{Sr}/^{86}\text{Sr}$  ratio which is different from that which has been

TABLE III

K-Ar data

Samples		K <sub>2</sub> O (%)	Ar* (%)	<sup>40</sup> Ar* (10 <sup>-6</sup> cm <sup>3</sup> g <sup>-1</sup> STP)	Age (Ma ± 2σ)
E198H	w.r.	5.00	89.55	105.6	559.0 ± 13.2
	0.2 μm	6.58	93.95	71.4	308.7 ± 6.9
	0.5-0.2 μm	5.84	95.24	116.4	531.8 ± 11.7
	1-0.5 μm	6.04	96.50	134.2	583.9 ± 12.7
	2-1 μm	6.21	97.84	137.3	581.6 ± 12.8
E220K	w.r.	2.20	85.23	47.6	571.2 ± 14.6
	1-0.5 μm	5.08	95.31	100.9	530.4 ± 11.9
	2-1 μm	4.69	97.40	105.1	588.0 ± 13.0
E220S	w.r.	4.45	93.39	97.0	574.5 ± 14.0
	0.2 μm	6.68	91.88	81.6	344.0 ± 7.9
	0.5-0.2 μm	6.53	96.94	133.2	542.5 ± 12.0
	1-0.5 μm	7.34	99.15	157.7	567.4 ± 11.9
	1-0.5 μm (II)	7.34	97.74	162.5	582.0 ± 12.4
	2-1 μm	7.43	98.70	161.7	573.6 ± 12.6
E220U	w.r.	2.84	78.91	52.2	495.8 ± 16.6
	2-1 μm	5.39	97.40	115.7	566.7 ± 12.4
E220Y	1-0.5 μm	5.59	97.39	121.0	571.1 ± 12.4
	2-1 μm	6.41	98.13	137.9	568.1 ± 12.2

w.r. = Whole rock; (II) is a duplicate.

Ar\* = Radiogenic argon.

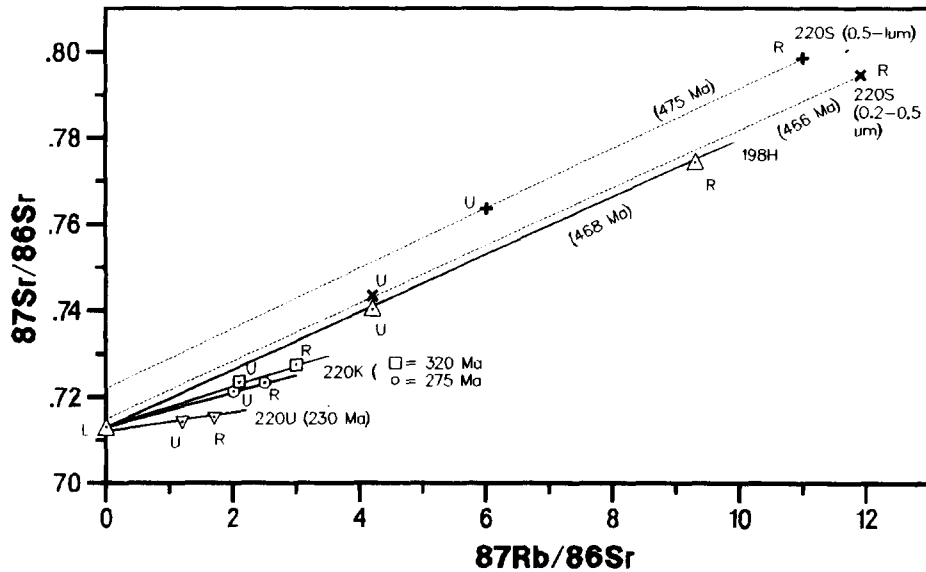


Fig. 7. Rb-Sr isochron diagram of the leaching experiments on the clay fractions. U = Unleached, R = residue after leaching, L = leachate.

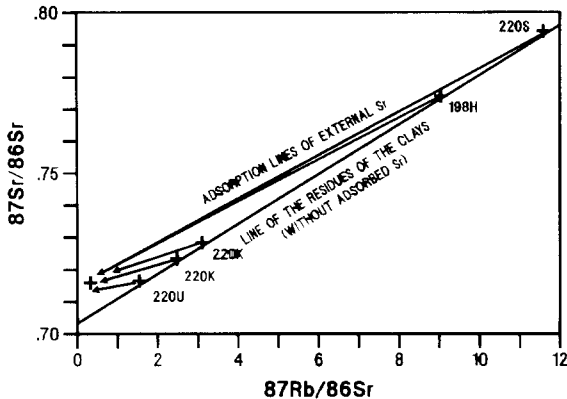


Fig. 8. Schematic explanation for the mixing line of the untreated clay fractions.

trapped in the clay minerals during their crystallization or further reset. Removal of that external Sr, which had artificially increased the slope of the regression line of the clay minerals to a value of  $643 \pm 16$  Ma, enables another regression line through almost all residues with a date of  $524 \pm 17$  Ma for initial  $^{87}\text{Sr}/^{86}\text{Sr}$  ratio of  $0.70357 \pm 0.00066$  (Fig. 8). Figure 8 also shows how adsorption of external Sr might have modified the slope of the initial isochron to an artificial regression line.

#### *Evolution of Hammamat Series*

The Rb–Sr and K–Ar isotopic data on whole rocks and mineral fractions of Hammamat samples lead to the following conclusions about the evolution of the Hammamat Series:

(1) At  $\sim 585$  Ma ago, the Hammamat sedimentary sequence was deposited from reworked juvenile material delivered from a narrowly defined area or metamorphosed during plutonic and volcanic activities occurring in the region. In the latter case, fluids producing calcite deposits migrated through the sequence.

(2) At  $\sim 530$  Ma ago, the Hammamat was reset by a metamorphic event of greenschist facies intensity, which might be a far echo of Caledonian plutonic activities affecting Europe to the north. If this event produced the first reset

of the sequence, then the calcite veins would represent the fluid activity during this period.

(3) After this metamorphic event, interstitial fluids with a fairly enriched  $^{87}\text{Sr}/^{86}\text{Sr}$  migrated throughout the sequence, inducing adsorption of that Sr onto the clay particles.

(4) Two low K–Ar apparent ages at  $\sim 326 \pm 18$  Ma are enigmatic. No technical influence can be considered because control by the Rb–Sr method could not be made owing to the lack of sample.

The geochemical and geochronologic results of the Hammamat Series enable a better understanding of the sources of these sediments and the timing of sedimentation and subsequent thermal events. An important aspect of the petrological study is that the source material of the Hammamat changed rapidly with time. Grothaus et al. (1979) argued, on the basis of a lack of quartz enrichment, that the Hammamat sediments were locally derived and deposited within small isolated basins. This would limit the applicability of our results if the Hammamat Series did not manifest similar lithologic characteristics everywhere in the Eastern Desert, as outlined in the introduction. The conclusion of Grothaus et al. (1979) that the Hammamat sediments were deposited in isolated basins means that limited sedimentary fractionation occurred, which allows us to use the composition of the Hammamat to reconstruct the composition of uppermost crust draining into this basin.

The upper part of the Hammamat was predominantly derived from reworking of the 600–575 Ma bimodal igneous rocks of the Northeastern Desert. This is shown not only by the results of the geochemical studies of the present study area, but by studies of the variation in clast lithologies carried out elsewhere in the Eastern Desert (Hafez and Abdel-Khalek, 1972). Within the upper part of the section, the Pink Granites became an increasingly important source towards the top. It is possible that our 'Average Hammamat Sediment' composi-

tion is biased by a progressive upsection variation in the proportion of Dokhan Volcanics and Pink Granite contribution, but our geochemical data do not allow us to resolve this question. Also, because our results agree with those of Noweir and El-Din (1979), we argue that the AHS listed in Table I is an appropriate representation of these sediments.

The composition of the upper half of the Hammamat section is very similar to the average composition of the modern upper continental crust (e.g., Taylor, 1977; Taylor and McLennan, 1981). These authors argue that the mean upper continental crust (UCC) contains 66% SiO<sub>2</sub>, 3.3% K<sub>2</sub>O, and 110 ppm Rb, with a K/Rb=250. The AHS is very similar in composition to the UCC: 65.2% SiO<sub>2</sub>, 3.0% K<sub>2</sub>O and 79 ppm Rb, with K/Rb=317. Thus the composition of the upper crust within this drainage basin was essentially identical to modern upper continental crust. This contrasts with the composition of the source of the lower half of the section. As previously noted, this source was probably similar to that of older ensimatic terranes to the south. Although the coarse clast size of these breccias led to our omitting these rocks from our geochemical studies, it is clear that the source of these breccias was much more mafic (~55% SiO<sub>2</sub>) and LIL-depleted (~1.5% K<sub>2</sub>O, K/Rb~500) than that of the younger Hammamat sediments.

These changes in the composition of the source of the Hammamat sediments manifest the evolution of the crust in the Northeastern Desert. Sedimentation rates for the Hammamat cannot at present be established; sedimentation rates for analogous Phanerozoic rift and successive basins range from 0.06 to 0.4 mm a<sup>-1</sup> with a mean of 0.14 mm a<sup>-1</sup> (Schwab, 1976). Using this average, the Hammamat in the study area could have been deposited in <3 × 10<sup>6</sup> a. This indicates a very rapid change in the composition of the source region, a manifestation of: (a) the onset of LIL-enriched bimodal igneous activity (Dokhan Volcanics and Pink Granite; Stern and Gottfried, 1986), and (b)

the complete burial or lateral removal by rifting and subsidence of the older, more mafic source terrane. The Hammamat sediments of the study area thus were deposited during a period reflecting rapid and profound changes in the crustal evolution of northeastern Africa.

The results of the Rb–Sr and K–Ar investigations are consistent with this interpretation. In a previous section, we argued that the Hammamat cannot be much older than ~600 Ma, nor much younger than ~590 Ma. The whole rock Rb–Sr date of 585 ± 15 Ma is thus close to the age of sedimentation. This is close to the end of the Precambrian, as it is presently defined as 590–530 Ma (Harland et al., 1982; Odin et al., 1982; Palmer, 1983; Plumb and James, 1986). It is not possible for the Rb–Sr whole-rock dates of clastic sediments to correspond to the time of sedimentation because the Rb–Sr isotopic signature of detrital grains was not reset at this time (Bonhomme, 1982; Clauer, 1982). Instead, the measured age corresponds either to the provenance or to first-generation metamorphic components. Mineral compositions have indeed been altered in the Hammamat sediments as a result of low-grade metamorphism and so have reset a part of the Rb–Sr system, but the first-generation illites may have retained their isotopic signature. The coarser clay fractions have retained their K–Ar signature at ~575 Ma; the intermediate-sized clay fractions have very similar K–Ar and Rb–Sr ages at 535 ± 5 and 524 ± 17 Ma. The whole rocks were probably able to form a regression line even though they are a mixture of components of different ages because the Rb–Sr whole-rock system seems to have remained closed during the 530 Ma event, which was not the case for the K–Ar whole-rock system. It can also be argued that because these sediments were largely reworked from young igneous rocks that solidified very shortly before erosion and deposition and had a similar low initial <sup>87</sup>Sr/<sup>86</sup>Sr ratio at this time, the regression line date of Fig. 5 is probably indistinguishable from the sedimentation age. The low initial <sup>87</sup>Sr/<sup>86</sup>Sr thus

corresponds fairly well to an average initial ratio for the source terrane at the time of sedimentation.

The low-grade metamorphic event at  $\sim 530$  Ma found in the clay fractions of the Hammamat seems to represent a lateral manifestation of a final pulse of alkaline magmatism concentrated in northernmost Egypt (Stern and Hedge, 1985) and southern Israel and Jordan (Segev, 1987). The K–Ar apparent ages at  $326 \pm 18$  Ma for the very small clay particles are more difficult to interpret as no thermal event is known in the region at this time, although a mild late Paleozoic diastrophism has been noted in the Western Desert of Egypt (Aadland and Schamel, 1987). It should also be mentioned that most igneous rocks from the region give K–Ar whole-rock ages in the range 570–430 Ma (Schurmann, 1966; Davies et al., 1980; Halpern and Tristan, 1981; Savino, 1982). Since all igneous activity in the region predates 540 Ma and nearly all predates 570 Ma (Stern and Hedge, 1985), their K–Ar dates have been reset. Possibly the range of values younger than 530 Ma represents the loss of radiogenic  $^{40}\text{Ar}$  during a late Paleozoic thermal event which has yet to be identified.

## Conclusions

The late Precambrian Hammamat sediments of Egypt preserve the detritus shed during a rapid and efficient episode of continental crust formation. Our geochemical and geochronologic studies of a single 400 m section led us to the following conclusions:

(1) The section studied is divisible into two parts: the lower half is composed of massive polymict breccias; the upper half of the section is composed of sandstones, siltstones and shales.

(2) The lower breccias were derived from the rapid uplift and erosion of a nearby 'ensimatic' terrane similar to that now preserved in the Central Eastern Desert to the south.

(3) The composition of the upper part of the Hammamat is similar to that of the upper con-

tinental crust, with 65%  $\text{SiO}_2$ , 3%  $\text{K}_2\text{O}$ ,  $\text{K/Rb} = 320$ , and  $(\text{Ce/Yb})_n = 10$ .

(4) The upper half of the section was predominantly derived from rapid reworking of 600–575 Ma bimodal igneous rocks with a ratio of andesites to granites of  $\sim 3:1$ .

(5) Rb–Sr whole-rock analyses give an age of  $585 \pm 15$  Ma that approximates the time of sedimentation. This age has also been determined on the coarser clay fractions by the K–Ar method. The initial  $^{87}\text{Sr}/^{86}\text{Sr}$  of  $0.70323 \pm 0.00013$  for the whole rocks indicates that the source region, in spite of being LIL-enriched, is juvenile.

(6) Rb–Sr analyses of leached fine fractions of the siltstones and shales give a regression line date of  $524 \pm 17$  Ma, which has been confirmed by K–Ar determinations at  $535 \pm 5$  Ma. This age is interpreted as the effect of a low-grade metamorphic imprint probably related to magmatic activity in this region during the Late Precambrian.

## Acknowledgments

Fieldwork in Egypt was made possible by a collaborative research program led by Professor W.H. Kanes (U. South Carolina, U.S.A.) and Professor E.M. El Shazly (Nuclear Materials Corporation, Egypt) and funded by the U.S. National Science Foundation (INT-7801469). Laboratory studies at UTD were funded under NSF grant EAR-8205802 to R.J. Stern. The authors sincerely appreciate the assistance of S. Mansour in the field and thank A. Hassan for drawing their attention to the geochemical studies of Noweir and El-Din. The authors would like to thank R.A. Wendling and R. Winkler for technical assistance during the K–Ar determinations, and are grateful to B. Mukhabadhyay and Arco Research Lab for providing guidance in sample preparation techniques. Finally, the authors would especially like to thank Diann Brackin, Darrell Queen, and Sun Exploration and Production Company for

their help and support in the preparation of this manuscript. This is UTD Programs in Geosciences contribution no. 527.

## References

- Aadland, R.K. and Schamel, S., 1987. Post-Paleozoic evolution of the northeast African shelf margin, Libya and Egypt. *Geol. Soc. Am., Abstr. with program*, 19: 565.
- Abuzeid, H.T., 1984. Geology of the Wadi Hamrawin area, Red Sea Hills, Eastern Desert, Egypt. Ph.D. Dissertation, Univ. South Carolina, Columbia, SC, 206 pp. (unpublished).
- Andrew, G., 1939. The greywackes of the Eastern Desert of Egypt. *Inst. Egypte, Bull.*, 21: 153-190.
- Barthoux, J., 1922. Chronologie et description des roches ignées du désert arabe. *Mém. Inst. Egypte*, 5: 262 pp.
- Bonhomme, M., 1982. The use of Rb-Sr and K-Ar dating methods as a stratigraphic tool applied to sedimentary rocks and minerals. *Precambrian Res.*, 18: 5-25.
- Bonhomme, M., Thuizat, R., Pinault, Y., Clauer, N., Wendling, A. and Winkler, R., 1975. Methode de datation potassium-argon. Appareillage et technique. *Notes tech. Inst. Geol. Univ. L. Pasteur, Strasbourg*, 3, 53 pp.
- Clauer, N., 1982. The rubidium-strontium method applied to sediments: certitudes and uncertainties. In: G.S. Odin (Editor), *Numerical Dating in Stratigraphy*. John Wiley, New York, pp. 245-276.
- Clauer, N., Giblin, P. and Lucas, J., 1984. Sr and Ar isotope studies of detrital smectites from the Atlantic Ocean (DSDP Legs 43, 48, and 50). *Isotope Geosci.*, 2: 141-151.
- Davies, J., Nairn, A.E.M. and Resselar, R., 1980. The paleomagnetism of certain Late Precambrian and Early Paleozoic rocks from the Red Sea Hills, Eastern Desert, Egypt. *J. Geophys. Res.*, 85: 3699-3710.
- Dunoyer de Segonzac, G., 1970. The transformation of clay minerals during diagenesis and low-grade metamorphism: A review. *Sediment.*, 15: 281-346.
- El Ramly, M.F., 1972. A new geologic map for the basement rocks in the eastern and southwestern deserts of Egypt. *Annals Geol. Surv. Egypt*, 2: 1-18.
- Gass, I.G., 1977. The evolution of the Pan African crystalline basement in NE Africa and Arabia. *J. Geol. Soc. London*, 134: 129-138.
- Ghanem, M., Dardir, A.A., Francis, M.H., Zalata, A.A. and Abu Zeid, K.M., 1973. Basement rocks in Eastern Desert of Egypt north of latitude 16°40' N. *Annals Geol. Surv. Egypt*, 3: 33-38.
- Ghobrial, M.G. and Lotfi, M., 1967. The geology of Gebel Gattar and Gebel Dokhan areas. *Geol. Surv. Egypt*, 40, 26 pp.
- Grothaus, B., Eppler, D. and Ehrlich, R., 1979. Depositional environment and structural implications of the Hammamat Formation, Egypt. *Annals Geol. Surv. Egypt*, 9: 564-590.
- Hafez, A. and Abdel-Khalek, M.L., 1972. Stratigraphy and correlation of the Hammamat conglomerates, Wadi Dib, Eastern Desert. *Bull. Fac. Sci., Cairo Univ.*, 44: 231-245.
- Halpern, M. and Tristan, N., 1981. Geochronology of the Arabian-Nubian Shield in southern Israel and eastern Sinai. *J. Geol.*, 89: 639-648.
- Harland, W.B., Cox, A.V., Llewellyn, P.G., Pickton, C.A., Smith, A.G. and Walters, R., 1982. *A Geologic Time Scale*. Cambridge University Press, Cambridge, 131 pp.
- Hume, W.F., 1934. *Geology of Egypt, Vol. 2, part I. The Metamorphic Rocks*. Geol. Surv. Egypt, 293 pp.
- Kröner, A., 1984. Late Precambrian plate tectonics and orogeny: A need to redefine the term Pan-African. In: J. Klerkx and J. Michot (Editors), *African Geology. Mus. R. Afr. Centr., Tervuren, (Belg.)*, pp. 24-28.
- Kröner, A., 1985. Ophiolites and the evolution of tectonic boundaries in the late Proterozoic Arabian-Nubian Shield of northeast Africa and Arabia. *Precambrian Res.*, 27: 277-300.
- Kubler, B., 1966. La cristallinité de l'illite et les zones tout à fait supérieures du métamorphisme. *Colloque sur les étages tectoniques. Univ. Neuchatel, A la Baconnière Ed., Neuchatel*, pp. 105-122.
- Massey, K.W., 1984. Rubidium-strontium geochronology and petrography of the Hammamat formation in the Northeastern Desert of Egypt. M.S. Thesis, Univ. Texas at Dallas, 77 pp. (unpublished).
- Morton, J.P. and Long, L.E., 1982. Rb-Sr ages of Precambrian sedimentary rocks in the U.S.A. *Precambrian Res.*, 18: 133-138.
- Noweir, A.M. and El-Din, S.A.S., 1979. Petrochemistry and geochemistry of the Dokhan Volcanics-Igla Formation of the Hammamat District, Eastern Desert, Egypt. *Delta J. Sci.*, 3: 91-106.
- Odin, G.S., Curry, D., Gale, N.H. and Kennedy, W.J., 1982. The Phanerozoic time scale in 1981. In G.S. Odin (Editor), *Numerical Dating in Stratigraphy, Vol. 2*. John Wiley, New York, pp. 957-960.
- Palmer, A.R., 1983. The decade of North American geology. 1983 geologic time scale. *Geology*, 11: 504-505.
- Pettijohn, F.J., 1957. *Sedimentary Rocks*. 2nd edition. Harper, New York, 719 pp.
- Plumb, K.A. and James, H.L., 1986. Subdivision of Precambrian time: Recommendations and suggestions by the Subcommittee on Precambrian stratigraphy. *Precambrian Res.*, 32: 65-92.
- Resselar, R. and Monrad, J.R., 1983. Chemical composition and tectonic setting of the Dokhan Volcanic Formation, Eastern Desert, Egypt. *J. African Earth Sci.*, 1: 103-112.
- Ries, A.C., Shackleton, R.M., Graham, R.H. and Fitches, W.R., 1983. Pan-African structures, ophiolites and melange in the Eastern Desert of Egypt: A traverse at 26° N. *J. Geol. Soc. London*, 140: 75-95.
- Savino, D., 1982. Paleomagnetic studies of some dikes from

- Esh el Mellaha Range (Eastern Desert, Egypt). M.S. Thesis, Univ. S. Carolina, Columbia, SC, 60 pp. (unpublished).
- Schürmann, H.M.E., 1966. The Pre-Cambrian along the Gulf of Suez and the northern part of the Red Sea. Leiden, E.J. Brill, 404 pp.
- Schwab, F.L., 1976. Modern and ancient sedimentary basins: comparative accumulation rates. *Geology*, 4: 723-727.
- Segev, A., 1987. The age of the latest Precambrian volcanism in southern Israel, northeastern Sinai, and southwestern Jordan — A re-evaluation. *Precambrian Res.*, 36: 277-285.
- Sims, P.K. and James, H.L., 1984. Banded iron-formation of late Proterozoic age in the Central Eastern Desert, Egypt: Geology and tectonic setting. *Econ. Geol.*, 79: 1777-1784.
- Steiger, R.H. and Jäger, E., 1977. Subcommittee on geochronology: Convention on the use of decay constants in geo- and cosmochronology. *Earth Planet. Sci. Lett.*, 36: 359-362.
- Stern, R.J., 1981. Petrogenesis and tectonic setting of Late Precambrian ensimatic volcanic rocks, Central Eastern Desert of Egypt. *Precambrian Res.*, 16: 197-232.
- Stern, R.J., 1985. The Najd Fault System of Saudi Arabia and Egypt: A late Precambrian rift-related transform system? *Tectonics*, 4,5: 497-511.
- Stern, R.J. and Gottfried, D., 1986. Petrogenesis of a late Precambrian (575-600 Ma) bimodal suite in northeast Africa. *Contrib. Mineral. Petrol.*, 92: 492-501.
- Stern, R.J. and Hedge, C.E., 1985. Geochronologic and isotopic constraints on late Precambrian crustal evolution in the Eastern Desert of Egypt. *Am. J. Sci.*, 285: 97-127.
- Stern, R.J., Gottfried, D.G. and Hedge, C.E., 1984. Late Precambrian rifting and crustal evolution in the Northeastern Desert of Egypt. *Geology*, 12: 168-172.
- Stoeser, D.B. and Camp, V.E., 1985. Pan-African microplate accretion of the Arabian Shield. *Geol. Soc. Am. Bull.*, 96: 817-826.
- Taylor, S.R., 1977. Island arc models and the composition of the continental crust. In: M. Talwani and W.C. Pitman III (Editors), *Island Arcs, Deep-Sea Trenches and Back-Arc Basins*. Am. Geophys. Union, Washington, DC, pp. 325-335.
- Taylor, S.R. and McLennan, S.M., 1981. The composition and evolution of the continental crust: Rare earth element evidence from sedimentary rocks. *Phil. Trans. R. Soc. Lond.*, 301: 381-399.
- Thiry, M., 1974. Technique de préparation des minéraux en vue de l'analyse aux rayons x. Rapport interne de Centre de Sédimentologie et Géochimie de la Surface, 25 pp.
- Weaver, C.E., 1956. The distribution and identification of mixed-layers in sedimentary rocks. *Am. Mineral.*, 41: 202-221.
- Wright, T.L. and Doherty, P.C., 1970. A linear programming and least squares computer method for solving petrologic mixing problems. *Geol. Soc. Am. Bull.*, 81: 1995-2008.
- York, D., 1966. Least squares fitting of a straight line. *Can. J. Phys.*, 44: 1079-1086.